

Synthesis and characterization of $\text{Ba}_{2-x}\text{Sr}_x\text{EuSbO}_6$ ceramic substrates for YBCO films

T. G. N. BABU, P. R. S. WARRIER, J. KURIAN, A. D. DAMODARAN, J. KOSHY*

Regional Research Laboratory (CSIR), Trivandrum 695019, India

A group of complex perovskites, $\text{Ba}_{2-x}\text{Sr}_x\text{EuSbO}_6$ (where $x = 0, 1$ and 2) was synthesized and sintered as single-phase materials for their use as substrates for YBCO superconductor films. These compounds have a complex cubic perovskite ($\text{A}_2\text{BB}'\text{O}_6$) crystal structure with lattice constant in the range 0.85–0.83 nm. The values of dielectric constant and loss factor of $\text{Ba}_{2-x}\text{Sr}_x\text{EuSbO}_6$ compounds are in the range suitable for their use as substrates for microwave applications of superconductor films. The dielectric constant decreases with increase of strontium content. No chemical reaction was observed between YBCO and $\text{Ba}_{2-x}\text{Sr}_x\text{EuSbO}_6$ ceramics even when they were mixed in composites of the form 80 vol % YBCO–20 vol % $\text{Ba}_{2-x}\text{Sr}_x\text{EuSbO}_6$ and processed under severe heat treatment. Addition of up to 20 vol % $\text{Ba}_{2-x}\text{Sr}_x\text{EuSbO}_6$ to YBCO showed no detrimental effect on superconducting properties of YBCO. The YBCO thick films developed on sintered specimens by dip coating were textured and showed (00 l) orientation with $T_{c(0)} = 92$ K.

1. Introduction

Recent breakthroughs in the development of superconducting thin films and their use in electronic devices, etc., have opened up a new area of research in the exploration of potential substrates for superconducting thick and thin films [1,2]. The substrate plays a vital role in the development of good quantity superconducting films with high critical current density. Many compounds, for example, sapphire, ZrO_2 , SrTiO_3 , MgO and LaAlO_3 , are in use as substrates for YBCO superconducting films [1,3–6]. Attempts have been made to develop substrate materials with all the potential quantities of an ideal substrate for microwave applications of YBCO superconducting films. In this context, compounds such as $\text{Ba}_2\text{DySnO}_{5.5}$, [7], REGaO_3 [8] and $\text{Ba}_2\text{GdNbO}_6$ [9] are worth mentioning. Here, we report the synthesis, characterization, and sintering of $\text{Ba}_{2-x}\text{Sr}_x\text{EuSbO}_6$ compounds, and their suitability as potential substrates for YBCO films.

2. Experimental procedure

The $\text{Ba}_{2-x}\text{Sr}_x\text{EuSbO}_6$ compounds (where $x = 0, 1$ and 2) were synthesized by the solid-state reaction method. Stoichiometric amounts of high-purity (99.9%) Eu_2O_3 , BaCO_3 , SrCO_3 and Sb_2O_3 were thoroughly ground to a homogeneous mixture in acetone medium. The mixture was pressed into pellets

and calcined in air at 1273 K for 36 h with two intermediate grindings. The calcined material was then finely ground and pelletized at a pressure of 5 ton cm^{-2} in the form of circular discs of 13 mm diameter and 1–2 mm thickness. These pellets were then sintered in air at 1773–1823 K for 16 h. Addition of up to 1 wt % cerium oxide and copper oxide was attempted in order to sinter these materials at lower temperatures. The bulk density of the sintered specimens was measured by Archimedes' method.

The phase purity of the samples was checked by powder X-ray diffraction (XRD) method using a Rigaku X-ray diffractometer with nickel-filtered CuK_α radiation. Differential thermal analysis (DTA) of sintered specimens was carried out to examine whether these compounds undergo phase transitions in the temperature range 300–1400 K using a Sieko TG/DTA Instrument (Model SSC/5200H, Seiko Instruments Inc., Japan). The stability and degradation of $\text{Ba}_{2-x}\text{Sr}_x\text{EuSbO}_6$ compounds were investigated by electrical resistivity and density measurements. For this, humidity treatment was carried out by keeping the sintered specimens in boiling water for a few hours. Density and electrical resistivity of the materials were measured before and after the humidity treatment. Electrical resistivity measurements were taken using the standard four-probe method with a Keithley current source (Model 220), Keithley nanovoltmeter (Model 181) and calibrated copper constant

* Author to whom all correspondence should be addressed.

thermocouple with an accuracy of ± 1 K. The values of dielectric constant and loss factor were measured using an HP 4192A Complex Impedance Analyser in the frequency range 30 Hz to 13 MHz at 77 and 300 K, with silver electrodes on both sides of the disc. Melting experiments were also carried out on $\text{Ba}_{2-x}\text{Sr}_x\text{EuSbO}_6$ powder in a platinum crucible. These samples were found to melt ~ 2050 K. Thus melted samples were quenched in air and examined by XRD technique.

$\text{YBa}_2\text{Cu}_3\text{O}_{7-\delta}$ (YBCO), freshly prepared by the solid-state reaction method, was used for preparation of YBCO– $\text{Ba}_{2-x}\text{Sr}_x\text{EuSbO}_6$ composites and YBCO thick-film paste. The 80 vol % YBCO–20 vol % $\text{Ba}_{2-x}\text{Sr}_x\text{EuSbO}_6$ composites were prepared and pressed in the form of circular pellets of dimensions 13 mm diameter and 1–3 mm thickness. The pressed pellets were then heated in air at 1223 K for 15 h followed by 20 h annealing at 773 K, and furnace cooled slowly. Thick-film paste of YBCO was prepared by mixing superconducting YBCO with isopropyl alcohol. The viscosity of the paste was controlled by addition of commercially available fish oil. The YBCO thick films were developed on sintered, highly polished $\text{Ba}_{2-x}\text{Sr}_x\text{EuSbO}_6$ substrates by dip coating. Heat treatment of the thick films was then carried out in a programmable furnace at a heating rate of 10 K min^{-1} to 1293 K, soaking for 1–3 min and cooling at a rate of 10 K min^{-1} to 1213 K and holding at the temperature for 2–4 h. The thick films were then annealed at 773 K in oxygen for 30 h. Slow cooling and annealing at 773 K facilitates oxygenation. All the composites and YBCO thick films on different substrates were processed under identical conditions, characterized by XRD, and their superconducting zero resistance transition temperature determined by electrical resistivity.

3. Results and discussion

The XRD patterns of sintered $\text{Ba}_{2-x}\text{Sr}_x\text{EuSbO}_6$ ($x = 0, 1$ and 2) for 2θ values between 10° and 90° are shown in Fig. 1 and the X-ray data are given in Table I. It is clear from Fig. 1 that $\text{Ba}_{2-x}\text{Sr}_x\text{EuSbO}_6$ compounds show similar crystal structure, as judged by the similarity in line positions. However, XRD line positions steadily shifted to higher 2θ values as barium was replaced by strontium. These compounds were also found to be isostructural with other rare-earth cubic perovskites with the general formula $\text{A}_2\text{BB}'\text{O}_6$ such as $\text{Ba}_2\text{GdNbO}_6$ and $\text{Ba}_2\text{PrSbO}_6$ compounds reported in the literature [9–13], in which doubling of the basic perovskites unit cell was observed. The ordering of the B and B' ions on the octahedral sites caused the doubling of the basic perovskite unit cell in $\text{Ba}_{2-x}\text{Sr}_x\text{EuSbO}_6$ compounds, which is characterized by the presence of superstructure lines in their XRD patterns. In addition, the substitution of strontium for barium (up to total replacement) has not caused any structural changes in cubic perovskite unit cell, and the XRD pattern of $\text{Sr}_2\text{EuSbO}_6$ was found to be similar to that of $\text{Ba}_2\text{EuSbO}_6$ (Fig. 1). This is due to the fact that preferential occupation of Sr^{2+} ions at

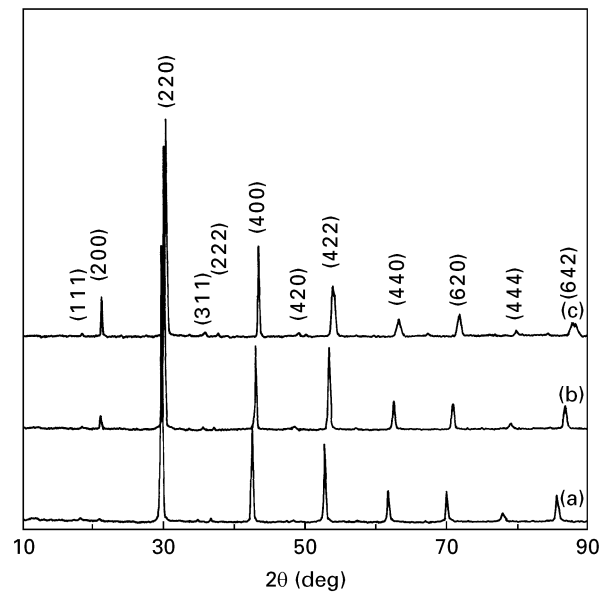


Figure 1 X-ray powder diffraction patterns of $\text{Ba}_{2-x}\text{Sr}_x\text{EuSbO}_6$ ceramics. (a) $x = 0$, (b) $x = 1$ and (c) $x = 2$.

TABLE I X-ray diffraction data for $\text{Ba}_2\text{EuSbO}_6$, BaSrEuSbO_6 and $\text{Sr}_2\text{EuSbO}_6$

	Serial	2θ (deg)	Width	d (nm)	I/I_0	hkl
$\text{Ba}_2\text{EuSbO}_6$	1	17.950	0.195	0.4938	3	111
	2	20.810	0.225	0.4265	3	200
	3	29.660	0.330	0.3010	100	220
	4	35.020	0.209	0.2560	3	311
	5	36.520	0.300	0.2458	4	222
	6	42.490	0.375	0.2126	41	400
	7	47.860	0.180	0.1899	3	420
	8	52.730	0.465	0.1735	32	422
	9	61.710	0.270	0.1502	14	440
	10	69.990	0.240	0.1343	13	620
	11	77.850	0.285	0.1226	5	444
	12	85.500	0.255	0.1135	12	642
BaSrEuSbO_6	1	18.300	0.200	0.4844	3	111
	2	21.200	0.300	0.4188	8	200
	3	30.150	0.390	0.2962	100	220
	4	35.400	0.202	0.2534	4	311
	5	37.100	0.210	0.2421	4	222
	6	43.120	0.390	0.2096	32	400
	7	48.430	0.208	0.1878	5	420
	8	53.490	0.540	0.1712	31	422
	9	62.520	0.540	0.1484	12	440
	10	70.910	0.300	0.1328	12	620
	11	79.150	0.210	0.1209	5	444
	12	86.790	0.340	0.1121	11	642
$\text{Sr}_2\text{EuSbO}_6$	1	18.510	0.225	0.4789	3	111
	2	21.430	0.315	0.4143	22	200
	3	30.490	0.600	0.2929	100	220
	4	36.010	0.330	0.2492	7	311
	5	37.550	0.280	0.2393	6	222
	6	43.620	0.390	0.2073	44	400
	7	49.020	0.255	0.1857	8	420
	8	54.380	0.270	0.1686	24	422
	9	63.450	0.255	0.1465	13	440
	10	71.820	0.240	0.1313	12	620
	11	79.670	0.200	0.1203	4	444
	12	87.380	0.225	0.1105	10	642

barium sites favours the formation of these compounds. Lattice parameter, a , was determined by a simple least-square fit computer program using all the observed XRD line positions for 2θ values 10° – 90° .

TABLE II Values of lattice constant, theoretical density and bulk density for $\text{Ba}_{2-x}\text{Sr}_x\text{EuSbO}_6$

Compound	Lattice constant (nm)	Theoretical density (g cm^{-3})	Bulk density (g cm^{-3})
$\text{Ba}_2\text{EuSbO}_6$	0.8555	6.96	6.75
BaSrEuSbO_6	0.8406	6.64	6.39
$\text{Sr}_2\text{EuSbO}_6$	0.8303	6.32	6.08

The lattice parameter decreased steadily with the increase of strontium for barium and was in the range 0.8505–0.8303 nm. This is due to the fact that Ba^{2+} ions were replaced by relatively smaller Sr^{2+} ions [14], resulting in a decrease in lattice parameter. The $\text{Ba}_2\text{EuSbO}_6$ compound was reported in the literature and the other two, BaSrEuSbO_6 and $\text{Sr}_2\text{EuSbO}_6$, are compounds, which are not reported in literature.

The theoretical density of $\text{Ba}_{2-x}\text{Sr}_x\text{EuSbO}_6$ compounds calculated from the lattice parameter, the sintered density determined by Archimedes' method and the lattice parameter, are given in Table II. It is noted that the increase in the strontium content for barium improved sinterability of $\text{Ba}_{2-x}\text{Sr}_x\text{EuSbO}_6$ ceramics. A similar result was also observed in some dielectric materials [15]. Addition of up to 1 wt % cerium oxide or copper oxide favoured sintering of these materials slightly at lower temperatures. However, their dielectric properties were affected and higher values of dielectric constant and loss factor were observed. These ceramics did not show any phase transitions up to 1373 K as observed by DTA measurements. The resistivity of sintered $\text{Ba}_{2-x}\text{Sr}_x\text{EuSbO}_6$ pellets was $\sim 10^{10} \Omega \text{ cm}$ at room temperature. Sintered $\text{Ba}_{2-x}\text{Sr}_x\text{EuSbO}_6$ specimens were highly stable under atmospheric conditions and showed no degradation even when they were kept in boiling water. The electrical resistivity and density of the humidity-treated specimens measured after drying, were the same as those of sintered $\text{Ba}_{2-x}\text{Sr}_x\text{EuSbO}_6$ specimens. Sintered specimens exhibited high mechanical strength and could be sliced into thin pieces, 0.5 mm thick, with a diamond cutter. Good reflecting surfaces were obtained by mechanical polishing and organic solvents such as alcohol, acetone and carbon tetrachloride were used as effective cleaning agents.

The values of dielectric constant, ϵ' , and loss factor, $\tan \delta$, of $\text{Ba}_{2-x}\text{Sr}_x\text{EuSbO}_6$ specimens were measured in the frequency range from 30 Hz to 13 MHz at 77 and 300 K. The plots of variation of ϵ' and $\tan \delta$ as a function of frequency are given in Figs 2 and 3, respectively. Table III gives the values of ϵ' and $\tan \delta$ at 10 MHz frequency at 77 K for these compounds. It is clear from Table III that values of dielectric constant and loss factor for $\text{Ba}_{2-x}\text{Sr}_x\text{EuSbO}_6$ compounds are comparable to those of commonly used substrates such as MgO and LaAlO_3 . The dielectric constant decreased with increase in strontium content in $\text{Ba}_{2-x}\text{Sr}_x\text{EuSbO}_6$ ceramics (Table III). This may be due to the fact that substitution of strontium at the barium sites decreases the unit cell size and hence

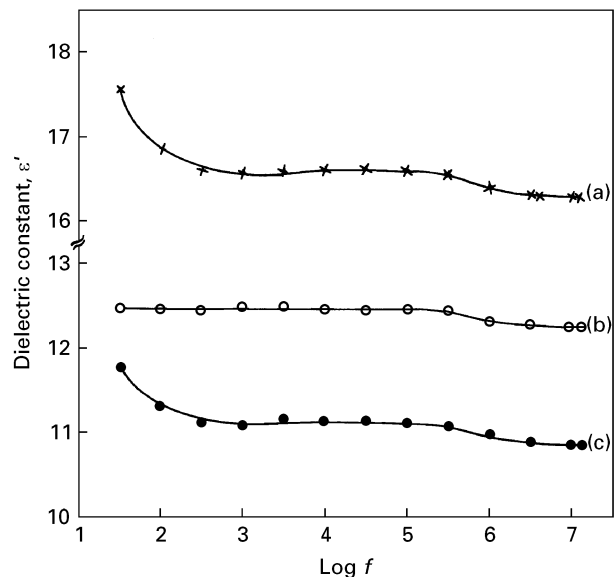


Figure 2 Variation of dielectric constant with frequency, f , for $\text{Ba}_{2-x}\text{Sr}_x\text{EuSbO}_6$ compounds at 77 K. (a) $x = 0$, (b) $x = 1$ and (c) $x = 2$.

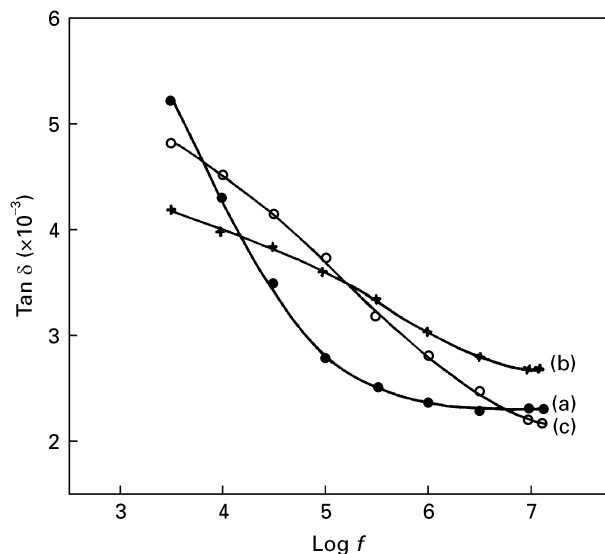


Figure 3 Variation of loss factor with frequency, f , for $\text{Ba}_{2-x}\text{Sr}_x\text{EuSbO}_6$ compounds at 77 K. (a) $x = 0$, (b) $x = 1$ and (c) $x = 2$.

TABLE III Values of dielectric constant and loss factor at 10 MHz frequency at 77 K for $\text{Ba}_{2-x}\text{Sr}_x\text{EuSbO}_6$

Compound	Dielectric constant, ϵ'	Loss factor, $\tan \delta$
$\text{Ba}_2\text{EuSbO}_6$	16.3	0.0023
BaSrEuSbO_6	12.3	0.0027
$\text{Sr}_2\text{EuSbO}_6$	10.8	0.0022

polarization is reduced. A similar result was also observed in $(\text{A}_{0.5}^{+1}\text{A}_{0.5}^{5+})\text{TiO}_3$ compounds [16].

One of the important criteria for the epitaxial growth of YBCO superconducting films on single-crystal substrates, is the lattice matching of the substrate with YBCO. Although lattice matching of these

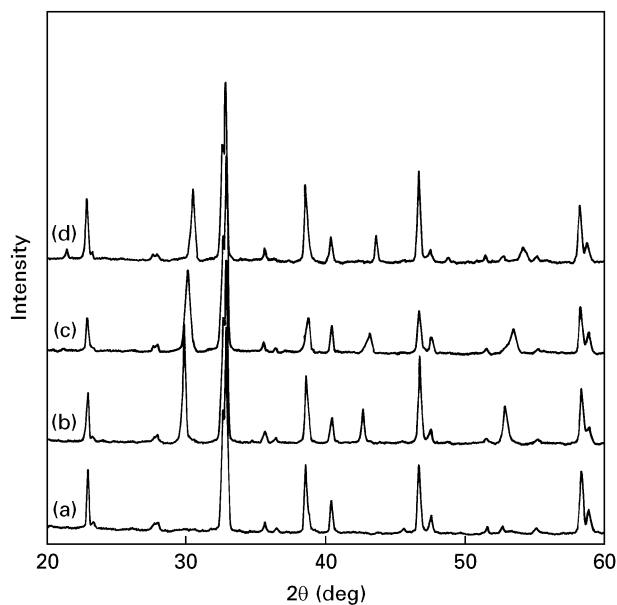


Figure 4 X-ray powder diffraction patterns of (a) pure YBCO, (b) 80 vol % YBCO–20 vol % $\text{Ba}_2\text{EuSbO}_6$, (c) 80 vol % YBCO–20 vol % BaSrEuSbO_6 and (d) 80 vol % YBCO–20 vol % $\text{Sr}_2\text{EuSbO}_6$. All composites were processed under identical conditions.

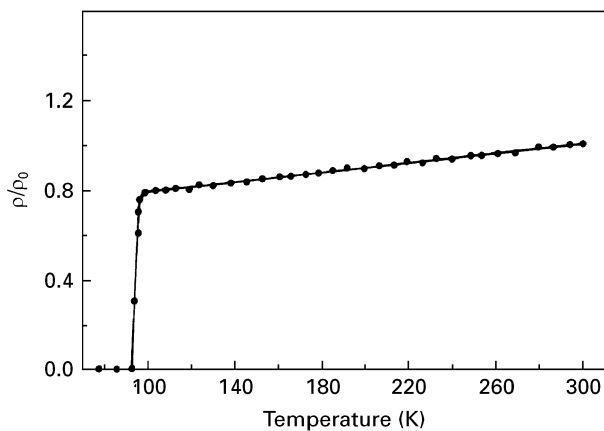


Figure 5 Temperature versus normalized resistivity curve for 80 vol % YBCO–20 vol % $\text{Sr}_2\text{EuSbO}_6$ composite. ρ_0 = room temperature resistivity; ρ = resistivity at temperature.

materials with YBCO is not perfect (Table II), taking into account the doubling of the perovskite unit cell, lattice constant values of $\text{Ba}_{2-x}\text{Sr}_x\text{EuSbO}_6$ are in a range comparable to that of MgO ($a = 0.4208$ nm) and LaAlO_3 ($a = 0.379$ nm), which are extensively used substrates for epitaxial growth of YBCO thin films. Melting experiments were also carried out to ascertain whether these compounds were stable upon melting. The XRD patterns recorded on melted and subsequently quenched $\text{Ba}_{2-x}\text{Sr}_x\text{EuSbO}_6$ specimens were identical to those of the sintered samples. This indicated that these materials melt congruently and single crystals could be grown from the melt. Detailed studies of single-crystal growth of $\text{Ba}_{2-x}\text{Sr}_x\text{EuSbO}_6$ are in progress.

The chemical non-reactivity of the substrate material with the superconductor film at the processing temperature is another important factor in the growth

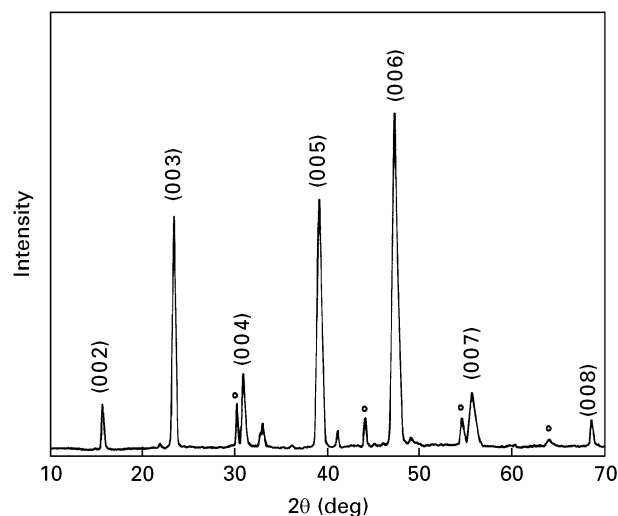


Figure 6 X-ray diffraction pattern of YBCO thick film on $\text{Sr}_2\text{EuSbO}_6$ substrate. Substrate peaks are marked by "o".

of YBCO films. To establish this fact, the chemical reactivity of $\text{Ba}_{2-x}\text{Sr}_x\text{EuSbO}_6$ with YBCO was studied at temperatures up to 1223 K. The composites of 80 vol % YBCO–20 vol % $\text{Ba}_{2-x}\text{Sr}_x\text{EuSbO}_6$ (where $x = 0, 1$ and 2) were prepared and annealed in air at 1223 K. The XRD patterns of the heat-treated composites and pure YBCO are given in Fig. 4. It was found that the composites showed no extra intensities due to the formation of impurity phases, but only the characteristic peaks of the substrate and the orthorhombic YBCO crystalline phases. This reveals that YBCO shows no chemical reaction with $\text{Ba}_{2-x}\text{Sr}_x\text{EuSbO}_6$ ceramics. All composites showed a superconducting zero resistance transition at 92 K with a transition width of 3 K. Fig. 5 shows the temperature versus normalized resistivity plot for a representative example. It indicates that the substantial addition of $\text{Ba}_{2-x}\text{Sr}_x\text{EuSbO}_6$ in YBCO did not show any detrimental effect on the superconducting properties of YBCO even after severe heat treatment.

The suitability of $\text{Ba}_{2-x}\text{Sr}_x\text{EuSbO}_6$ ceramics as substrates for YBCO superconductor was investigated by developing a YBCO thick film on these substrate materials by dip coating. The XRD pattern of YBCO thick film developed on $\text{Sr}_2\text{EuSbO}_6$ is shown in Fig. 6 as a typical example. The thick film showed (00 l) orientation due to the orthorhombic YBCO in addition to the characteristic peaks of the substrate. High-temperature processing (1293 K) caused partial melting and texturing of the thick film, similar to YBCO thin films. A superconducting zero resistance was observed at 92 K for the thick films developed on $\text{Ba}_{2-x}\text{Sr}_x\text{EuSbO}_6$ (where $x = 0, 1$ and 2) substrates. Temperature versus resistance plot for a representative YBCO thick film is shown in Fig. 7. A peel-off test, carried out using a highly adhesive tape, confirmed the excellent adhesion of YBCO thick film to the substrate. Although $\text{Ba}_{2-x}\text{Sr}_x\text{EuSbO}_6$ ceramics were polycrystalline in nature, the development of YBCO thick films on sintered, polished specimens, signifies their potential use as substrate materials for YBCO

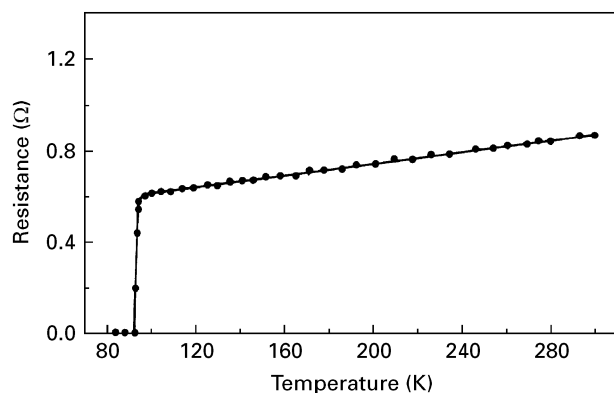


Figure 7 Temperature versus resistance curve for YBCO thick film on $\text{Sr}_2\text{EuSbO}_6$ substrate.

superconducting thin films. Work is in progress for the epitaxial growth of YBCO thin films by the laser ablation method.

4. Conclusion

The $\text{Ba}_{2-x}\text{Sr}_x\text{EuSbO}_6$ (where $x = 0, 1$ and 2) ceramics were synthesized, characterized and sintered as single-phase materials by the solid-state reaction method. The BaSrEuSbO_6 and $\text{Sr}_2\text{EuSbO}_6$ were new compounds to be reported. All these materials were found to be isostructural and have ordered cubic perovskite structure of $\text{A}_2\text{BB}'\text{O}_6$ type compounds. The values of dielectric constant and loss factor of sintered $\text{Ba}_{2-x}\text{Sr}_x\text{EuSbO}_6$ specimens were in the range comparable to those of commercially available single crystals, such as MgO and LaAlO_3 . They melt congruently and growth of single crystals from their melts is possible. These materials showed no chemical reaction with YBCO superconductor and substantial addition up to 20 vol % did not affect the superconducting properties of YBCO. Thick films of YBCO

developed on these substrates by dip coating showed (001) orientation and $T_{c(0)}$ of 92 K.

Acknowledgements

T. G. N. Babu and J. Kurian thank the Council of Scientific and Industrial Research, New Delhi, for the financial assistance.

References

1. E. K. HOLLMANN, O. G. VENDIK, A. G. ZAITSEV and B. T. MELEKH, *Supercond. Sci. Technol.* **7** (1994) 609.
2. J. E. NORDMAN, *ibid.* **8** (1995) 681.
3. J. GAO, B. B. G. KLOPMAN, W. A. M. AAMINK, A. E. REITSMA, G. J. GERITSMA and H. ROGALLA, *J. Appl. Phys.* **71** (1992) 2333.
4. A. ODAGAWA and Y. ENOMOTO, *Phys. C* **248** (1995) 162.
5. L. DIMESSO, O. B. HYUN and I. HIRABAYASHI, *ibid.* **248** (1995) 127.
6. D. H. KIM, W. N. KANG, Y. H. KIM, J. H. PARK, J. J. LEE, G. H. YI, T. S. HAHN and S. S. CHOI, *ibid.* **246** (1995) 235.
7. J. KOSHY, K. S. KUMAR, J. KURIAN, Y. P. YADAVA and A. D. DAMODARAN, *ibid.* **234** (1994) 211.
8. C. KLEMENZ and H. J. SCHEEL, *J. Crystal Growth* **129** (1993) 421.
9. J. KOSHY, J. KURIAN, J. K. THOMAS, Y. P. YADAVA and A. D. DAMODARAN, *Jpn J. Appl. Phys.* **33** (1994) 117.
10. W. F. GALLASSO and W. DARBY, *J. Phys. Chem.* **66** (1962) 131.
11. X. ZHANG and Q. WANG, *J. Am. Ceram. Soc.* **74** (1991) 2846.
12. C. D. BRANDLE and V. J. FRATELLO, *J. Mater. Res.* **5** (1990) 2160.
13. J. KURIAN, J. KOSHY, P. R. S. WARRIER, Y. P. YADAVA and A. D. DAMODARAN, *J. Solid State Chem.* **116** (1995) 193.
14. R. D. SHANNON, *Acta Crystallogr.* **A32** (1976) 751.
15. M. TAKATA and K. KAGEYAMA, *J. Am. Ceram. Soc.* **72** (1989) 1955.
16. H. TAKAHASHI, Y. BABA, K. EZAKI, Y. OKAMOTO, K. SHIBATA, K. KUROKI and S. NAKANO, *J. Appl. Phys.* **30** (1991) 2339.

Received 23 February
and accepted 17 September 1996